

# A Two-Fluid Model for Herschel-Bulkley Fluid Flow through Narrow Tubes

Santhosh Nallapu\* and G. Radhakrishnamacharya

Department of Mathematics, National Institute of Technology,  
Warangal, India

## Abstract

A two-fluid model of Herschel-Bulkley fluid flow through tubes of small diameters is studied. It is assumed that the core region consists of Herschel-Bulkley fluid and Newtonian fluid in the peripheral region. The analytical solutions for velocity, flow flux, effective viscosity, core hematocrit and mean hematocrit have been derived and the effects of various relevant parameters on these flow variables have been studied. It is found that the effective viscosity, core hematocrit and mean hematocrit for Newtonian fluid is less than that for Bingham fluid, power-law fluid and Herschel-Bulkley fluid. It has been observed that the effective viscosity and mean hematocrit increase with yield stress, power-law index, hematocrit and tube radius but the core hematocrit decreases with hematocrit and tube radius. Further, it is also noticed that the flow exhibits the anomalous Fahraeus-Lindqvist effect.

**Key Words:** Effective Viscosity, Herschel-Bulkley Fluid, Hematocrit, Fahraeus-Lindqvist Effect, Yield Stress

## 1. Introduction

The word microcirculation represents the flow of blood through small blood vessels such as arterioles, capillaries and venules. It consists of the complex network of blood vessels whose diameter ranges from approximately 4–100  $\mu\text{m}$ . Further, the flow of blood through smaller diameter blood vessels is accompanied by anomalous effects. In particular, it has been observed that the apparent viscosity of blood increases with tube diameter and this is known as Fahraeus-Lindqvist effect. The hematocrit of blood within the tube is lower than that in the feed reservoir and this is called Fahraeus effect. These effects have been confirmed by several investigators.

It has been pointed out that for flow in smaller blood vessels at lower shear rates, the yield stress for the blood is non-zero and the blood behaves like a non-Newtonian

fluid [1,2]. Haynes [3] and Bugliarello and Sevilla [4] have considered a two-fluid model with both fluids as Newtonian fluids and with different viscosities. Sharan and Popel [5] and Srivastava [6] have reported that for blood flowing through narrow tubes, there is a peripheral layer of plasma and a core region of suspension of all erythrocytes. Haldar and Andersson [7] and Chaturani and Samy [8] have studied a two-layered blood flow model in which the core region is occupied by a Casson type fluid and peripheral region by Newtonian fluid. Chaturani and Upadhyaya [9,10] analyzed two-fluid models assuming Newtonian fluid in peripheral region and polar fluids in core region. Shukla et al. [11] have studied the two-layered models of blood flow through stenosed arteries.

Though Newtonian and several non-Newtonian models have been used to study the motion of blood, it is realized [12] that Herschel-Bulkley model describes the behaviour of blood very closely. Herschel-Bulkley fluids are a class of non-Newtonian fluids that require a finite

---

\*Corresponding author. E-mail: princenallapu@gmail.com

stress, known as yield stress, in order to deform. Therefore, these materials behave like rigid solids when the local shear is below the yield stress. Once the yield stress is exceeded, the material flows with a non-linear stress-strain relationship either as a shear-thickening fluid, or a shear-thinning one. Few examples of fluids behaving in this manner include paints, food products, plastics, slurries, pharmaceutical products etc.

Maruthi Prasad and Radhakrishnamacharya [13] discussed the steady flow of Herschel-Bulkley fluid in an inclined tube of non-uniform cross-section with multiple stenoses. Vajravelu et al. [14] studied a mathematical model for a Herschel-Bulkley fluid flow in an elastic tube. Sankar and Usil Lee [15] analyzed the two-fluid Herschel-Bulkley model for flow of blood in catheterized arteries. Vajravelu et al. [16] considered peristaltic transport of Herschel-Bulkley fluid in an inclined tube.

Recently, Santhosh and Radhakrishnamacharya [17] studied a two-fluid model for the flow of Jeffrey fluid through a porous medium in tubes of small diameters. In the present paper, a two-layered model is considered, in which the peripheral region consists of Newtonian fluid and the core region is represented by a Herschel-Bulkley fluid. Following the analysis of Chaturani and Upadhyaya [9] and Vajravelu et al. [14], the linearised equations of motion have been solved and analytical solution has been obtained. The analytical expressions for velocity, flow rate, effective viscosity, core hematocrit and mean hematocrit are obtained. The results are depicted graphically and the effects of various relevant parameters have been studied.

### 2. Formulation of the Problem

We consider the steady, laminar and axisymmetric flow of Herschel-Bulkley fluid through a narrow tube of uniform cross-section with constant radius ‘a’. It is assumed that the flow in the tube is represented by a two-layered model in which peripheral region of thickness  $\epsilon$  ( $a - b = \epsilon$ ) is occupied by Newtonian fluid and the other is a central core region of radius ‘b’, which is represented by Herschel-Bulkley fluid (Figure 1). Let  $\mu_p$  and  $\mu_c$  be the viscosities of the fluid in peripheral region and core region, respectively. The cylindrical coordinates ( $r, z$ ) are chosen, where  $r$  and  $z$  denote the radial and axial co-

ordinates and the  $z$  axis is taken along the axis of the tube.

The equations governing the flow of an incompressible Herschel-Bulkley fluid for the present problem (Maruthi Prasad and Radhakrishnamacharya [13] and Vajravelu et al. [14]) are given by:

$$\frac{1}{r} \frac{\partial}{\partial r} (r\tau_{rz}) = -\frac{\partial p}{\partial z} \tag{1}$$

where  $\tau_{rz}$ , the shear stress of the Herschel-Bulkley fluid, is given by

$$\tau_{rz} = \mu \left( -\frac{\partial u}{\partial r} \right)^n + \tau_0, \tau_{rz} \geq \tau_0 \tag{2}$$

$$\frac{\partial u}{\partial r} = 0, \tau_{rz} \leq \tau_0 \tag{3}$$

Here  $u$  is the axial velocity,  $p$  is the pressure,  $\tau_0$  is the yield stress,  $\mu$  is the consistency factor and  $n (\geq 1)$  is the flow behavior index and they represent the non-Newtonian effects.

The region between  $r = 0$  and  $r = r_0$  is called plug core region and in this region,  $\tau_{rz} \leq \tau_0$ . In the region between  $r = r_0$  and  $r = b$ , we have  $\tau_{rz} \geq \tau_0$ .

Let  $u = v_1(r)$  be the velocity in the peripheral region and  $v_2(r)$  in the core region. Then the equations governing the flow of fluid are [7,14]:

Peripheral region (Newtonian fluid):

$$\frac{\partial v_1}{\partial r} = -\frac{Pr}{2\mu_p} \text{ for } b \leq r \leq a \tag{4}$$

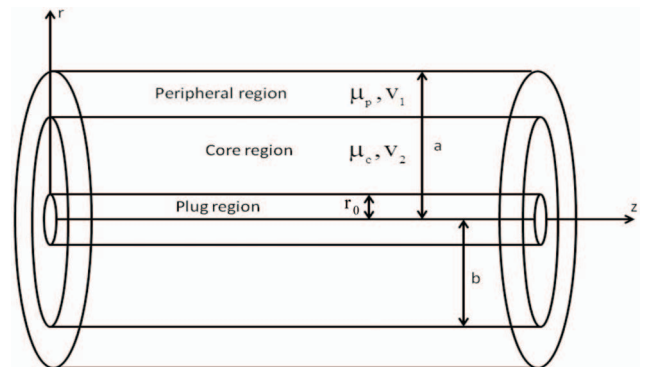


Figure 1. Geometry of the problem.

Core region (Herschel-Bulkley fluid):

$$\frac{\partial v_2}{\partial r} = -\left(\frac{P}{2\mu_c}\right)^{\frac{1}{n}}(r-r_0)^{\frac{1}{n}} \text{ for } r_0 \leq r \leq b \quad (5)$$

where  $P = -\frac{\partial p}{\partial z}$  is the constant pressure gradient.

The boundary conditions for the problem are:

$$v_1 = 0 \text{ at } r = a \quad (6a)$$

$$v_1 = v_2, \tau_1 = \tau_2 \text{ at } r = b \quad (6b)$$

$$\tau_{rz} \text{ is finite at } r = 0 \quad (6c)$$

Condition (6a) is the classical no-slip boundary condition for the velocity, (6b) denotes the continuity of velocities and stresses at the interface and (6c) is the regularity condition.

Solving equations (4) and (5) under the conditions (6), we get

$$v_1(r) = \frac{P}{4\mu_p}(a^2 - r^2) \text{ for } b \leq r \leq a \quad (7)$$

$$v_2(r) = \left(\frac{P}{2\mu_c}\right)^{\frac{1}{n}}\left(\frac{n}{n+1}\right)\left((b-r_0)^{1+\frac{1}{n}} - (r-r_0)^{1+\frac{1}{n}}\right) + \frac{P}{4\mu_p}(a^2 - b^2) \text{ for } r_0 \leq r \leq b \quad (8)$$

The expression for the fluid velocity in the plug flow region,  $v_p$ , is obtained by substituting  $r = r_0$  in Eq. (8) as

$$v_p(r) = \left(\frac{P}{2\mu_c}\right)^{\frac{1}{n}}\left(\frac{n}{n+1}\right)(b-r_0)^{1+\frac{1}{n}} + \frac{P}{4\mu_p}(a^2 - b^2) \quad (9)$$

for  $0 \leq r \leq r_0$

The flow flux in the peripheral region and core region, denoted by  $Q_p$  and  $Q_c$ , are given by

$$Q_p = 2\pi \int_b^a v_1(r) r \, dr \quad (10)$$

and

$$Q_c = \pi r_0^2 v_p(r) + 2\pi \int_{r_0}^b v_2(r) r \, dr \quad (11)$$

Substituting for  $v_1$ ,  $v_2$  and  $v_p$  from (7), (8) and (9) into (10) and (11), we get

$$Q_p = \frac{P\pi a^4}{8\mu_p}(1-d^2)^2 \quad (12)$$

and

$$Q_c = \frac{P\pi a^4}{8\mu_p} \left( \beta^{k-1} \left( \frac{4}{1+k} \right) \mu' d^{k+3} (1-\tau_p)^{k+1} \left( 1 - \frac{2\tau_p}{2+k} (1-\tau_p) - \frac{2}{3+k} (1-\tau_p)^2 \right) + 2d^2(1-d^2) \right) \quad (13)$$

where

$$k = \frac{1}{n}, \beta = \frac{Pa}{2\mu_c}, \mu' = \frac{\mu_p}{\mu_c}, d = \frac{b}{a}, \tau_p = \frac{r_0}{b} \quad (14)$$

Here  $d$  is the non-dimensional core radius.

Thus, the flow flux through the tube is given by

$$Q = Q_p + Q_c \quad (15)$$

Using (12) and (13) in (15), we get

$$Q = \frac{P\pi a^4}{8\mu_p} \left( 1-d^4 + \beta^{k-1} \left( \frac{4}{1+k} \right) \mu' d^{k+3} (1-\tau_p)^{k+1} \left( 1 - \frac{2\tau_p}{2+k} (1-\tau_p) - \frac{2}{3+k} (1-\tau_p)^2 \right) \right) \quad (16)$$

Comparing (16) with flow flux for Poiseuille's flow, we get the effective viscosity as

$$\mu_{eff} = \frac{\mu_p}{1-d^4 + \beta^{k-1} \left( \frac{4}{1+k} \right) \mu' d^{k+3} (1-\tau_p)^{k+1} \left( 1 - \frac{2\tau_p}{2+k} (1-\tau_p) - \frac{2}{3+k} (1-\tau_p)^2 \right)} \quad (17)$$

Here  $d$  is the non-dimensional core radius.

In the case when there is no yield stress, that is  $\tau_0 = 0$ , the Herschel-Bulkley model reduces to the power-law model. Thus, substituting  $\tau_0 = 0$  i.e.,  $\tau_p = 0$ , we obtain the

value of effective viscosity for the power-law model as

$$\mu_{eP} = \frac{\mu_p}{1 - d^4 + \beta^{k-1} \left( \frac{4}{3+k} \right) \mu' d^{k+3}} \quad (18)$$

Further, if we put  $k = 1$  in (18), we obtain results for Newtonian fluids, i.e.,

$$\mu_{eN} = \frac{\mu_p}{1 - d^4 + \mu' d^4} \quad (19)$$

This is same as the expression obtained by Buglierello and Sevilla [4].

### 2.1 Mean Hematocrit for Cell-free Wall Layer

The percentage volume of red blood cells is called the hematocrit and is approximately 40–45% for adult human beings.

The core hematocrit  $H_c$  is related to the hematocrit  $H_0$  of blood leaving or entering the tube by

$$H_0 Q = H_c Q_c \quad (20)$$

Substituting for  $Q_c$  and  $Q$  from (13) and (15) in (20), we get (after simplification),

$$\begin{aligned} \frac{\bar{H}_c}{H_0} = 1 & \\ + \frac{1 - 2d^2 + d^4}{\beta^{k-1} \alpha \left( \frac{4}{1+k} \right) d^{k+3} \left( (1 - \tau_p)^{k+1} - \frac{2\tau_p}{2+k} (1 - \tau_p)^{k+2} - \frac{2}{3+k} (1 - \tau_p)^{k+3} \right) + 2d^2 - 2d^4} & \end{aligned} \quad (21)$$

where  $\bar{H}_c$  is the normalized core hematocrit.

The mean hematocrit within the tube  $H_m$  is related to the core hematocrit  $H_c$  by

$$H_m \pi a^2 = H_c \pi b^2 \quad (22)$$

On simplification, we get

$$\frac{\bar{H}_m}{H_0} = \frac{H_m}{H_0} = \frac{H_c}{H_0} d^2 \quad (23)$$

where  $\bar{H}_m$  is the normalized mean hematocrit.

Substituting for  $\bar{H}_c$  from equation (21) in (23), we get

$$\bar{H}_m = d^2 \left( 1 + \frac{1 - 2d^2 + d^4}{\beta^{k-1} \alpha \left( \frac{4}{1+k} \right) d^{k+3} \left( (1 - \tau_p)^{k+1} - \frac{2\tau_p}{2+k} (1 - \tau_p)^{k+2} - \frac{2}{3+k} (1 - \tau_p)^{k+3} \right) + 2d^2 - 2d^4} \right) \quad (24)$$

### 3. Results and Discussion

The effects of yield stress, power-law index and hematocrit on effective viscosity  $\mu_{eff}$ , core hematocrit  $\bar{H}_c$  and mean hematocrit  $\bar{H}_m$ , have been numerically computed by using Mathematica software and the results are graphically presented in Figures 2–13. In the present analysis, the following values are chosen:  $\mu_p = 1.2$  centipoise (cp),  $\mu_c = 4.0$  cp and  $d = 1 - (\epsilon/a)$  in which  $\epsilon = 3.12 \mu$  for 40% hematocrit,  $3.60 \mu$  for 30% and  $4.67 \mu$  for 20% (Haynes [3], Chaturani and Upadhyya [9]).

The effects of various parameters on effective viscosity ( $\mu_{eff}$ ) are shown in Figures 2–5. It can be seen that the effective viscosity ( $\mu_{eff}$ ) for Newtonian fluid is less than that for Bingham fluid [ $n = 1, \tau_p \neq 0$ ], power-law fluid [ $n \neq 1, \tau_p = 0$ ] and Herschel-Bulkley fluid [ $n \neq 1, \tau_p \neq 1$ ] (Figure 2). Figures 3–5 show that the effective viscosity ( $\mu_{eff}$ ) increases with the yield stress ( $\tau_p$ ), power-law index ( $n$ ) and hematocrit ( $H_0$ ). The values of effec-

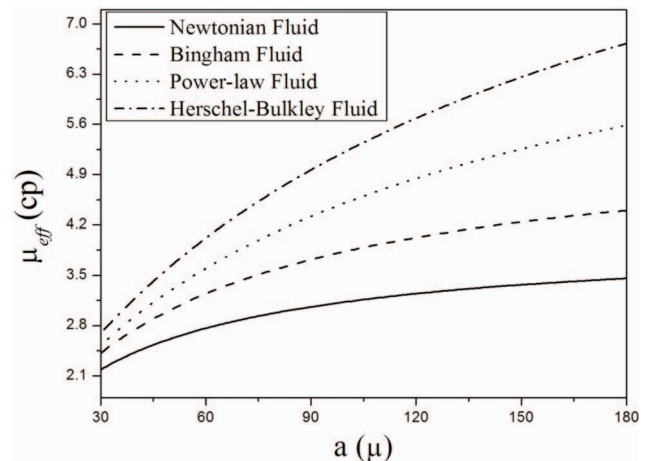


**Figure 2.** Variation of  $\mu_{eff}$  with tube radius ‘a’ for different fluids (Newtonian fluid [ $n = 1.0, \tau_p = 0$ ], Bingham fluid [ $n = 1, \tau_p \neq 0 (= 0.2)$ ], power-law fluid [ $n \neq 1 (= 1.1), \tau_p = 0$ ], Herschel-Bulkley fluid [ $n \neq 1 (= 1.1), \tau_p \neq 1 (= 0.2)$ ] and  $H_0 = 40\%$ ).

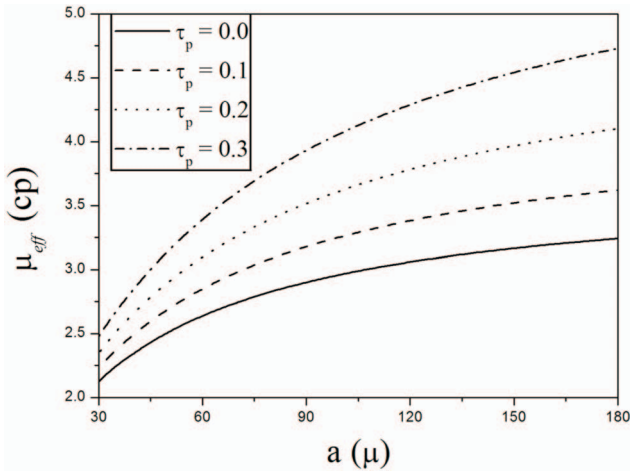


**Figure 3.** Effect of yield stress ( $\tau_p$ ) on  $\mu_{eff}$  ( $H_0 = 40\%$  and  $n = 1.05$ ).

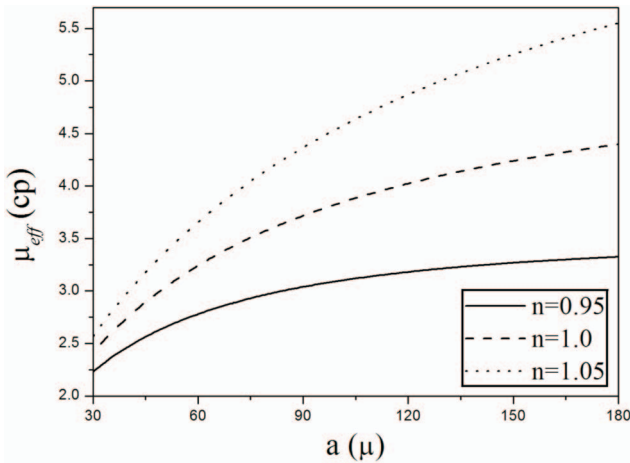


**Figure 4.** Effect of power-law index ( $n$ ) on  $\mu_{eff}$  ( $H_0 = 40\%$  and  $\tau_p = 0.2$ ).

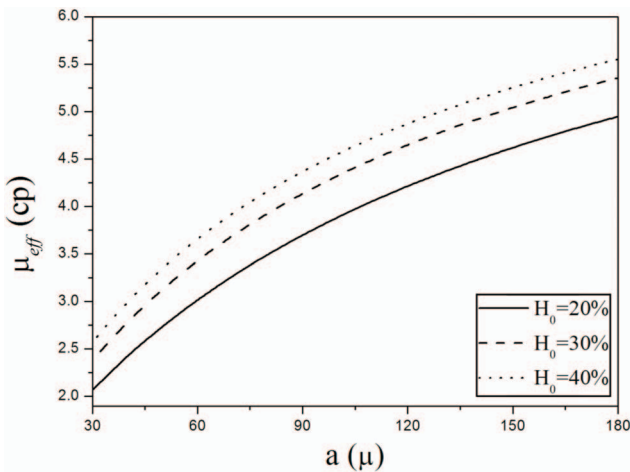


**Figure 5.** Effect of hematocrit ( $H_0$ ) on  $\mu_{eff}$  ( $n = 1.05$  and  $\tau_p = 0.2$ ).

Effective viscosity computed from the present model are in good agreement, within the acceptable range, with the corresponding values of the effective viscosity obtained in the theoretical models of Haynes [3], Sharan and Popel [5] and Chaturani and Upadhyya [9]. Further, for given values of yield stress ( $\tau_p$ ), power-law index ( $n$ ) and hematocrit ( $H_0$ ) the effective viscosity ( $\mu_{eff}$ ) increases with tube radius ( $a$ ) (Figures 2–5), i.e., the flow exhibits Fahrenaus-Lindqvist Effect.

Figures 6–13 display the effects of various parameters on the core hematocrit ( $\bar{H}_c$ ) and mean hematocrit ( $\bar{H}_m$ ). It is noticed that the core hematocrit ( $\bar{H}_c$ ) and

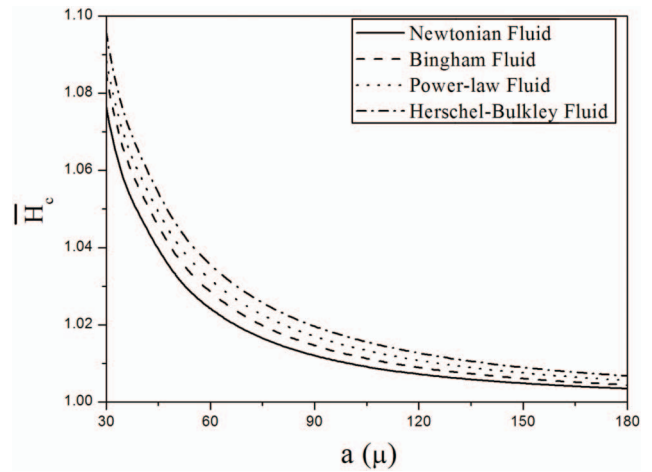


**Figure 6.** Effect of different fluids on  $\bar{H}_c$  with tube radius ‘a’ (Newtonian fluid [ $n = 1.0, \tau_p = 0$ ], Bingham fluid [ $n = 1, \tau_p \neq 0 (= 0.2)$ ], power-law fluid [ $n \neq 1 (= 1.1), \tau_p = 0$ ], Herschel-Bulkley fluid [ $n \neq 1 (= 1.1), \tau_p \neq 1 (= 0.2)$ ] and  $H_0 = 40\%$ ).

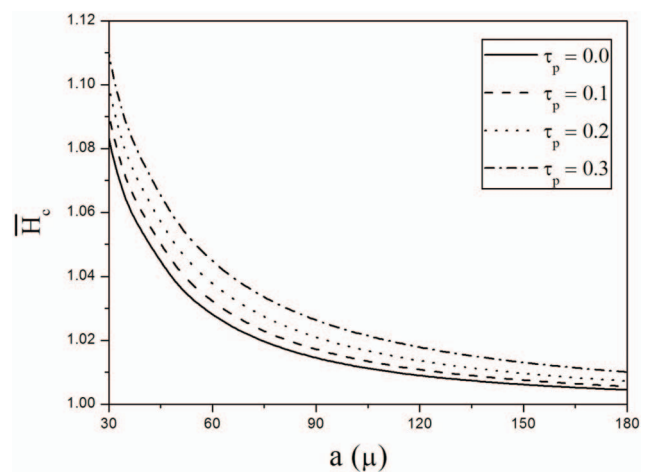


**Figure 7.** Effect of yield-stress ( $\tau_p$ ) on  $\bar{H}_c$  ( $H_0 = 40\%$  and  $n = 1.05$ ).



mean hematocrit ( $\bar{H}_m$ ) for Newtonian fluid is less than that all other fluids (Figures 6 and 10). Also, the core hematocrit ( $\bar{H}_c$ ) increases with yield stress ( $\tau_p$ ) (Figure 7) and power-law index ( $n$ ) (Figure 8) but decreases with hematocrit ( $H_0$ ) (Figure 9). It is seen that for given values of yield stress ( $\tau_p$ ), power-law index ( $n$ ) and hematocrit ( $H_0$ ), the core hematocrit ( $\bar{H}_c$ ) decreases with tube radius ( $a$ ) (Figures 6–9). It can be observed that the mean hematocrit ( $\bar{H}_m$ ) increases with yield stress ( $\tau_p$ ) (Figure 11), power-law index ( $n$ ) (Figure 12), hematocrit ( $H_0$ ) (Figure 13) and tube radius ( $a$ ) (Figures 10–13).

### 4. Conclusions

We have analyzed a two-fluid model for the steady

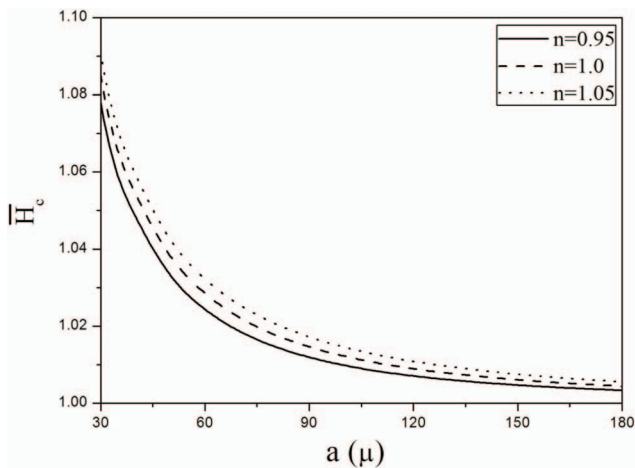


**Figure 8.** Effect of power-law index ( $n$ ) on  $\bar{H}_c$  ( $H_0 = 40\%$  and  $\tau_p = 0.2$ ).

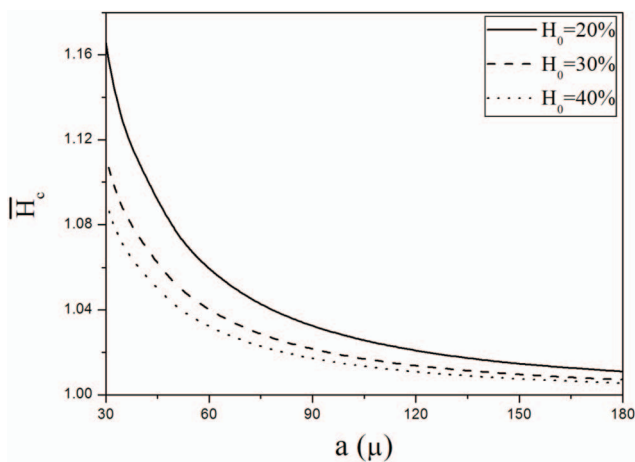


**Figure 9.** Effect of hematocrit ( $H_0$ ) on  $\bar{H}_c$  ( $n = 1.05$  and  $\tau_p = 0.2$ ).

flow of Herschel-Bulkley fluid through tubes of small diameters. With the assumption that there is Herschel-Bulkley fluid in core region and Newtonian fluid in peripheral region, analytical expressions for effective viscosity, core hematocrit and mean hematocrit are obtained. The effects of yield stress, power-law index and hematocrit on effective viscosity, core hematocrit and mean hematocrit have been studied. It is found that effective viscosity, core hematocrit and mean hematocrit of Newtonian fluid is less than that for Bingham fluid, power-law fluid and Herschel-Bulkley fluid. The effective viscosity increases with yield stress, power-law index, he-

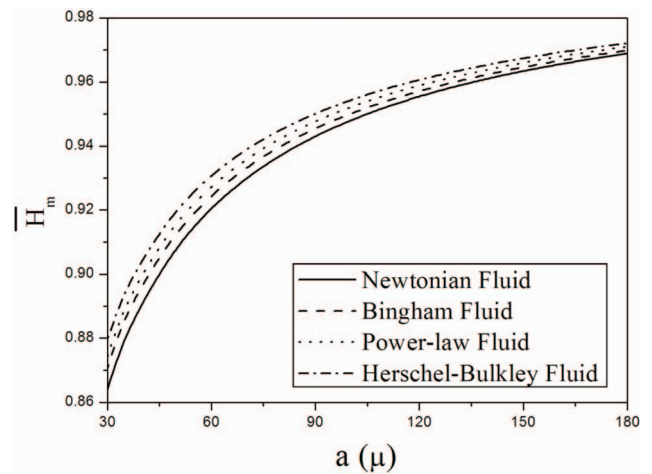


**Figure 10.** Effect of different fluids on  $\bar{H}_m$  with tube radius ‘a’ (Newtonian fluid [ $n = 1.0, \tau_p = 0$ ], Bingham fluid [ $n = 1, \tau_p \neq 0 (= 0.2)$ ], power-law fluid [ $n \neq 1 (= 1.1), \tau_p = 0$ ], Herschel-Bulkley fluid [ $n \neq 1 (= 1.1), \tau_p \neq 1 (= 0.2)$ ] and  $H_0 = 40\%$ ).

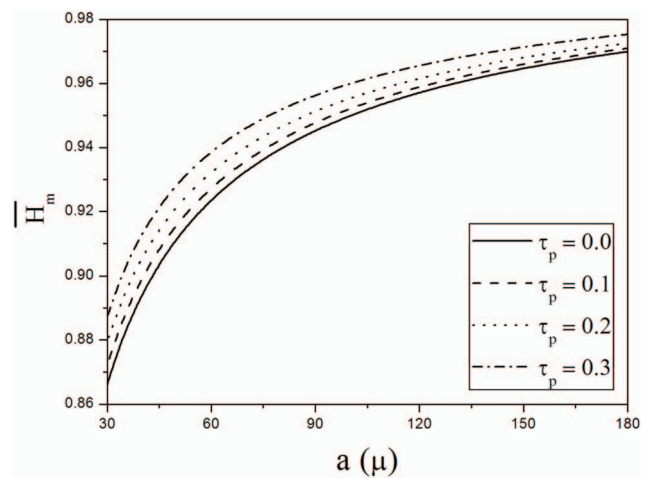


**Figure 11.** Effect of yield stress ( $\tau_p$ ) on  $\bar{H}_m$  ( $H_0 = 40\%$  and  $n = 1.05$ ).

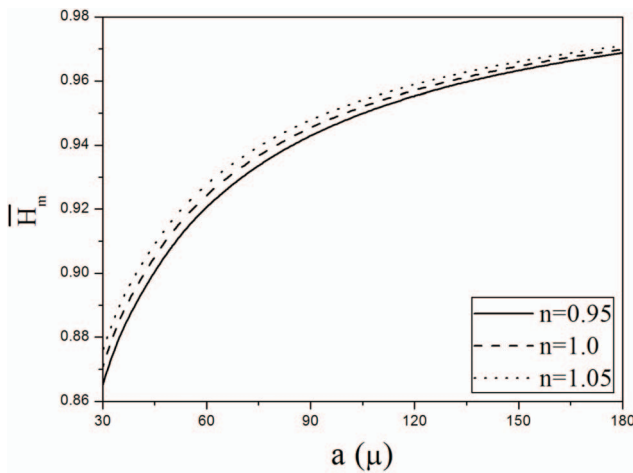


**Figure 12.** Effect of power-law index ( $n$ ) on  $\bar{H}_m$  ( $H_0 = 40\%$  and  $\tau_p = 0.2$ ).

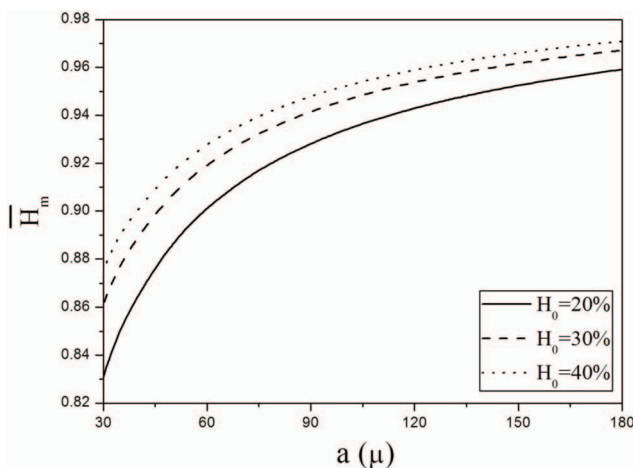


**Figure 13.** Effect of hematocrit ( $H_0$ ) on  $\bar{H}_m$  ( $n = 1.05$  and  $\tau_p = 0.2$ ).

matocrit and tube radius. Hence, the flow exhibits the anomalous Fahraeus-Lindqvist effect.

### References

- [1] Haynes, R. H. and Burton, A. C., "Role of Non-Newtonian Behaviour of Blood in Hemodynamics," *Am. J. Physiol.*, Vol. 197, p. 943 (1959).
- [2] Srivastava, V. P. and Saxena, M., "A Two-Fluid Model of Non-Newtonian Blood Flow Induced by Peristaltic Waves," *Rheol. Acta*, Vol. 34, No. 4, pp. 406–414 (1995). doi: 10.1007/BF00367155
- [3] Haynes, R. H., "Physical Basis of the Dependence of Blood Viscosity on Tube Radius," *Am. J. Physiol.*, Vol. 198, pp. 1193–1200 (1960).
- [4] Bugliarello, G. and Sevilla, J., "Velocity Distribution and other Characteristics of Steady and Pulsatile Blood Flow in Fine Glass Tubes," *Biorheology*, Vol. 7, pp. 85–107 (1970).
- [5] Sharan, M. and Popel, A. S., "A Two-phase Model for Flow of Blood in Narrow Tubes with Increased Effective Viscosity near the Wall," *Biorheology*, Vol. 38, pp. 415–428 (2001).
- [6] Srivastava, V. P., "A Theoretical Model for Blood Flow in Small Vessels," *Appl. Appl. Math.*, Vol. 2, pp. 51–65 (2007).
- [7] Haldar, K. and Andersson, H. I., "Two-layered Model of Blood Flow through Stenosed Arteries," *Acta Mech.*, Vol. 117, No. 1, pp. 221–228 (1996). doi: 10.1007/BF01181050
- [8] Chaturani, P. and Ponalagusamy, R., "Pulsatile Flow of Casson's Fluid through Stenosed Arteries with Applications to Blood Flow," *Biorheology*, Vol. 23, pp. 499–511 (1986).
- [9] Chaturani, P. and Upadhyaya, V. S., "On Micropolar Fluid Model for Blood Flow through Narrow Tubes," *Biorheology*, Vol. 16, pp. 419–428 (1979).
- [10] Chaturani, P. and Upadhyaya, V. S., "A Two-Fluid Model for Blood Flow through Small Diameter Tubes," *Biorheology*, Vol. 18, pp. 245–253 (1981).
- [11] Shukla, J. B., Parihar, R. S. and Gupta, S. P., "Effects of Peripheral Layer Viscosity on Blood Flow through the Artery with Mild Stenosis," *Bull. Math. Biol.*, Vol. 42, pp. 797–805 (1980). doi: 10.1016/S0092-8240(80)80003-6
- [12] Blair, G. W. S. and Spanner, D. C., "An Introduction to Biorheology," *Elsevier, Amsterdam*. (1974).
- [13] Maruthi Prasad, K. and Radhakrishnamacharya, G., "Flow of Herschel-Bulkley Fluid through an Inclined tube of Non-uniform Cross-section with Multiple Stenoses," *Arch. Mech.*, Vol. 60, No. 2, pp. 161–172 (2008).
- [14] Vajravelu, K., Sreenadh, S., Devaki, P. and Prasad K. V., "Mathematical Model for a Herschel-Bulkley Fluid Flow in an Elastic Tube," *Cent. Eur. J. Phys.*, Vol. 9, No. 5, pp. 1357–1365 (2011). doi: 10.2478/s11534-011-0034-3
- [15] Sankar, D. S. and Lee, U., "Two-fluid Herschel-Bulkley Model for Blood Flow in Catheterized Arteries," *J.*

- Mech. Sci. Tech.*, Vol. 22, pp. 1008–1018 (2008). doi: [10.1007/s12206-008-0123-4](https://doi.org/10.1007/s12206-008-0123-4)
- [16] Vajravelu, K., Sreenadh, S. and Ramesh Babu, V., “Peristaltic Transport of a Herschel-Bulkley Fluid in an Inclined Tube,” *Int. J. Non-Linear Mech.*, Vol. 40, No. 1, pp. 83–90 (2005). doi: [10.1016/j.ijnonlinmec.2004.07.001](https://doi.org/10.1016/j.ijnonlinmec.2004.07.001)
- [17] Santhosh, N., Radhakrishnamacharya, G. and Chamkha, A. J., “Flow of a Jeffrey Fluid Through a Porous Medium in Narrow Tubes,” *J. Por. Media.*, Vol. 18, No. 1, pp. 71–78 (2015). doi: [10.1615/JPorMedia.v18.i1.60](https://doi.org/10.1615/JPorMedia.v18.i1.60)

***Manuscript Received: Oct. 2, 2015***

***Accepted: May 5, 2016***